International Journal of Concrete Structures and Materials

RESEARCH

Open Access

Influence of Fly Ash and Slag on Combined Alkali-Silica Reaction and Corrosion of Steel in RC Structures

Williams Dunu[1,3*] and Mike Otieno[2,3]

Abstract

Supplementary cementitious materials (SCMs) utilized to attenuate steel corrosion or alkali-silica reaction (ASR) damage in concrete have not yet been investigated in the context of the combined action of the deterioration processes. This research examines the impact of fly ash and slag on the combined effect of steel corrosion and ASR on concrete structures. Concrete beams having fine aggregate susceptible to ASR (reactive) and fine aggregate not susceptible to ASR (non-reactive) with 20 mm concrete cover utilizing 100% PC, 50/50 PC/SL, and 70/30 PC/FA binders with a constant w/b ratio of 0.60. After 7 days of water curing and 20 days of air curing, beam specimens were exposed to three-cycle conditions for one week each; the beams were exposed to high humidity of 94 ± 3% in a storage tank at 38 ± 2 °C, wetting (with 5% NaCl) and air-drying cycles in the laboratory for 52 weeks. The specimens were monitored for expansion and corrosion evaluation tests at the completion of each humid exposure and wetting cycle. The results indicate that slag and fly ash in structures containing reactive aggregate exposed to chloride (combined effect) resulted in a higher rate of expansion and corrosion than specimens with non-reactive aggregate (aggregate not susceptible to ASR). Moreover, the 100% PC specimens with reactive aggregate exhibited a higher corrosion rate and expansion than the SCM specimens with reactive aggregate.

Keywords Corrosion, Alkali-silica reaction, Combined action, Reactive aggregate, SCMs

1 Introduction

Concrete is the most popular building material in the world (Williamson & Juenger, 2016). There are many reasons why concrete is the most common building material, including its durability, low relative cost, low maintenance, and great fire resistance (Parmar et al., 2019). However, prolonged exposure to an aggressive environmental condition can lead concrete to deteriorate. In addition, several factors, such as reinforcement corrosion, alkali-silica reaction (ASR), and carbonation, can impair the durability of concrete (Saha et al., 2018). Several studies (Leemann et al., 2014; Liu et al., 2018) have been conducted on minimizing ASR and corrosion in RC structures. However, most research on the mechanisms of degradation (steel corrosion and ASR) has been conducted independently. The partial substitution of Portland cement with supplementary cementitious materials (SCMs) in concrete substantially reduces alkalinity in the pore solution and ASR damage. However, limited research (Mazarei et al., 2017) has examined the impact of SCMs and ASR on time to corrosion initiation. Therefore, the number of deteriorated RC structures caused by the combined action of chloride-induced steel corrosion and alkali-silica reaction may continue to rise

Journal information: ISSN 1976-0485/eISSN 2234-1315.

*Correspondence:
Williams Dunu
msc8083dunu@gmail.com
[1] Department of Civil Engineering, Nusa Putra University, Sukabumi, Jawa Barat 43152, Indonesia
[2] School of Physics, Engineering & Computer Science, University of Hertfordshire, England, UK
[3] School of Civil and Environmental Engineering, University of the Witwatersrand, Johannesburg, South Africa

and continue to satisfy the durability and sustainability requirements of corrosion-affected RC structures beyond the initiation phase. From an economic and structural performance standpoint, information on the effect of SCMs on the alkali-silica reaction and corrosion propagation process is crucial.

Alkali-silica reaction refers to the reaction between the reactive silica in the aggregate and the alkaline pore solution of the concrete. Reactive aggregates, high alkalinity (pH $^{>}$ 11) in the pore solution, and high moisture content (> 80% relative humidity) are necessary for ASR to occur (Angulo-Ramírez et al., 2018). The reaction product (ASR gel) forms in and around aggregates, within the concrete's cracks, and within the matrix of the concrete paste. Moreover, the ASR gel is porous. It has a large surface area that can absorb moisture from the surrounding pore solution and environment, leading to concrete expansion and structural deterioration due to the formation of cracks.

Corrosion of steel reinforcement embedded in concrete has been regarded as the major threat to the durability of reinforced concrete structures. The entire lifespan (service life) consists primarily of two phases: corrosion initiation and corrosion propagation. Steel corrosion caused by chloride ingress or carbonation has been identified as the primary cause of durability failure and shortened service life in RC structures (Fang et al., 2006) For RC structures in marine environments where de-icing compounds are used, chloride-induced corrosion has been identified (Torres-Luque et al., 2014) as the leading cause of durability failure.

Otieno et al. (2010), Cho and Noh (2012), Kim and Olek (2016), Rutkauskas et al. (2017), Liaudat et al. (2018), among others, have looked into how to mitigate ASR and steel corrosion in concrete. Thomas (1996) examined a study that looked at what happened to pore solution pastes when fly ash and slag were added. This study shows that adding SCMs (like fly ash and slag) lowers the amount of alkali hydroxide in the pore solution of pastes, mortars, and concretes as the level of SCM replacement increases. Adding slag to concrete not only reduces the damage caused by ASR but also makes it last longer by making the matrix thicker and less porous. The thicker microstructure than Portland cement paste is made up of more capillary holes filled with low-density calcium silicate hydrate (C-S-H) gel. By binding chlorides, adding fly ash (FA) to concrete is also thought to be an effective way to prevent corrosion caused by chlorides in reinforced concrete structures. The higher chloride binding capacity of FA concrete can be explained by (i) the high alumina (Al_2O_3) content of FA, which makes more Friedel's salt, and (ii) the production of more gel during hydration, which makes it easier for chlorides to stick to the concrete physically (Otieno, 2013). In recent years, it has become standard to add SCMs to RC structures to make them durable. But a lot of study has already been done to find out how SCMs affect each mode of deterioration separately. Also, more study needs to be done to figure out how much fly ash and slag affect concrete structures with ASR in corrosive environments.

Concrete containing reactive silica aggregates is particularly vulnerable to alkali-silica reaction (ASR) when exposed to high alkaline pore solutions (pH $\geq$12), as noted by Heisig et al. (2016). The resulting expansive pressure from ASR can cause cracking in the concrete, potentially allowing chlorides to penetrate. Despite this, the corrosion mechanism resulting from the combined effects of chloride attack and ASR on steel reinforcement in concrete remains poorly understood. This study investigates the combined impact of chloride-induced corrosion and ASR on the durability of reinforced concrete structures in marine environments.

2 Materials and Method

This paper aims to assess the performance of the fly ash and slag on the combined action of alkali-silica reaction and chloride-induced steel corrosion in reinforced concrete structures. Currently, there is no standard test method available to monitor the combined effect of alkali-silica reaction and chloride-induced corrosion of steel on the performance of reinforced concrete structures. Therefore, this research includes monitoring specimens designed such that length change due to ASR and corrosion activity could be assessed. The specimens were designed based on the general requirements of (ASTM C1293, 2008).

This study utilized two types of fine aggregates: Sub-Nigel sand (washed crusher sand) from Nigel, Gauteng, classified as reactive aggregate, and andesite sand from Gauteng, considered non-reactive. The Sub-Nigel sand contains quartzite with a relative density of 2.77, water absorption of 0.4%, and dry aggregate crushing value (ACV) of 12.7%. The andesite sand contains granite with a relative density of 2.94, water absorption of 0.5%, and dry aggregate crushing value of 5.9% (AfriSam, 2017). The particle size distribution curves for both fine aggregates are presented in Fig. 1.

Both Nigel aggregate and andesite aggregate from the particle size distribution graph indicate that the fine aggregates used in the concrete mix are well graded.

The concretes used in this study were made using plain Portland cement (PC), fly ash (FA), and ground granulated blast furnace slag (SL) binders in the proportion 100 PC, 70/30 PC/FA, and 50/50 PC/SL using a w/b ratio of 0.60. The primary objective of this study is to investigate the combined effects of alkali-silica

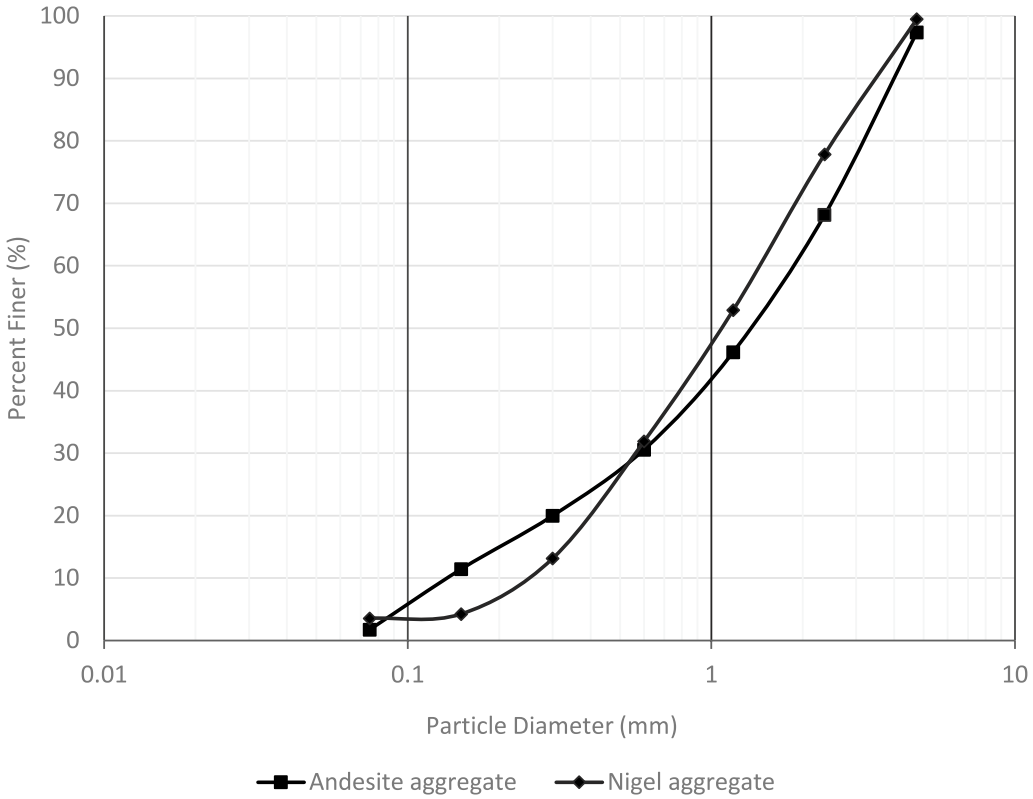

Fig. 1 Particle size distribution curve of fine aggregate

reaction (ASR) and corrosion on reinforced concrete structures, with a focus on the influence of different binder types. To achieve this, a w/b ratio of 0.60 was selected to increase the likelihood of deterioration within the study period. This approach allows to examine the interactions between ASR and corrosion under more aggressive conditions.

While varying w/b ratios would undoubtedly impact the study's outcomes, the primary focus remains on understanding the role of binder types in mitigating or exacerbating these deterioration mechanisms. Future studies could indeed explore the effects of different w/b ratios on the combined deterioration of RC structures. By using a higher w/b ratio, this may be simulating more severe exposure conditions or less optimized concrete mixtures. However, this choice does not undermine the validity of the findings regarding the influence of binder types on ASR and corrosion. These results provide valuable insights into the complex interactions between these deterioration mechanisms and can inform the development of more durable concrete mixtures for marine environments. The 50/50 PC/SL and 70/30 PC/FA cement blends were used because the replacement level is the most used in South Africa (SANS920, 2011).

Eighteen (18) concrete beams of size 150 × 150 × 500 mm were cast (6 beams each cast using concrete made of PC, PC/FA, and PC/SL binder). Three specimens contained fine reactive aggregate for each mixture, and three contained non-reactive fine aggregate. All specimens contained non-reactive coarse aggregate. The mixture identifications and proportions and the binders chemical analysis are shown in Tables 1 and 2, respectively. Sodium hydroxide (NaOH) was dissolved in the mixing water to bring the alkali content of the concrete mixture to 1.25% Na_2Oe by mass of cement as required in (ASTM C227-03, 1994; ASTM C1293, 2008).

A single high yield steel bar of 12 mm diameter and 498 mm long conforming to South African standard SANS 920 was embedded in each beam specimen. The reinforcement bars were covered with black insulation tape and epoxy coated (sikadur—31 DW epoxy sealant) on both ends to provide an effective exposed surface area of approximately 75 cm^2. While maintaining the cover depth (20 mm), the steel bars were placed in the cross-section centre (at a cover depth of 20 mm from each exposed face) of the beams exposed to chloride ingress (see Fig. 2b). In-built reservoirs are cast into

Table 1 Summary of concrete mix proportion

Mixture ID	PC	FA	SL	w/c	Water (kg/m^3)	Coarse aggregate	Fine aggregate	NaOH (kg.m^3)
PC (100) RS	375	–	–	0.6	225	994.12	778.37	4.59
PC (100) NRS	375	–	–	0.6	225	976.98	843.78	4.59
PC (70)/FA (30) RS	262.5	112.5	–	0.6	225	994.12	778.37	1.06
PC (70)/FA (30) NRS	262.5	112.5	–	0.6	225	976.98	843.78	1.06
PC (50)/SL (50) RS	187.5	–	187.5	0.6	225	994.12	764.52	0.29
PC (50)/SL (50) NRS	187.5	–	187.5	0.6	225	976.98	829.08	0.29

Table 2 Measured oxide composition of binders used

Oxide composition (%)	Portland cement	Slag	Fly ash
SiO_2	19.57	33.69	54.92
Al_2O_3	4.93	17.06	31.76
Fe_2O_3	2.64	0.65	3.41
MnO	0.37	0.97	0.04
MgO	2.06	9.79	1.18
SO_3	3.33	3.39	0.46
CaO	62.57	31.31	4.14
Na_2O	0.00	0.25	0.22
K_2O	0.45	0.98	0.78
TiO_2	0.35	0.84	1.61
P_2O_5	0.10	0.02	0.54
Cr_2O_3	0.03	0.01	0.05
NiO	0.00	0.00	0.01
LOI	3.60	1.35	0.81
Na_2Oe ($Na_2O + 0.658K_2O$)	0.2961	0.6943	0.5167

Oxide composition by XRF method

the beam specimens top (exposed face) for ponding the specimens with sodium chloride solution.

2.1 Concrete Specimens Curing and DEMEC Target Installation

All the specimens were cured in water at 23 ± 2 °C for 7 days and air-drying in the laboratory to simulate cases where concretes achieve their potential quality to penetrability (durability). This choice was informed by previous research (Khanzadeh-Moradllo et al., 2015), which suggests that prolonged curing can create a denser surface layer, potentially hindering chloride ion penetration and moisture ingress. By limiting the water curing duration to 7 days, the study aimed to increase the susceptibility of the specimens to chloride-induced corrosion and ASR. This approach allows to investigate the combined effects of these deterioration mechanisms under more aggressive conditions, which is relevant to real-world exposure scenarios.

The chosen curing regime may influence ASR and corrosion kinetics by facilitating the ingress of moisture and chloride ions, potentially accelerating the deterioration processes. This, in turn, enables us to study the interactions between ASR and corrosion within a relatively shorter timeframe. While standard 28-day water curing might have yielded different results, the curing regime is designed to simulate scenarios where concrete structures are exposed to environmental conditions that promote deterioration.

During the air-drying of the beam specimens, the DEMEC targets were fixed longitudinally on both sides of the beams at 50 mm intervals. In addition, the targets were also transversely arranged at 50 mm on the exposed face of the beam specimens (see Fig. 2a and c). This arrangement of the DEMEC targets monitors the expansion of the specimens in both directions. The beam specimens were not coated with epoxy to ensure sufficient moisture to cause ASR and corrosion (Mazarei et al., 2017; Trejo et al., 2017).

2.2 Exposure Regimes for Accelerated Corrosion and ASR Testing

After curing for 28 days, the beam specimens were exposed to three-cycle conditions for a 1-week each; specimens were subjected to 38 ± 2 °C temperature and 94 ± 3% relative humidity (ASTM C227-03, 1994; ASTM C1293, 2008) in a covered plastic container (water bath). The specimens were placed on the perforated plastic crates (supporting rack). The supporting rack did not act as a vapour barrier but provided the free movement of vapour within the container. The supporting rack was fixed at the height of 25 mm ± 5 mm above the surface of the water in the storing container to prevent the specimens from losing moisture, which is an essential component for ASR to occur, and to ensure that the

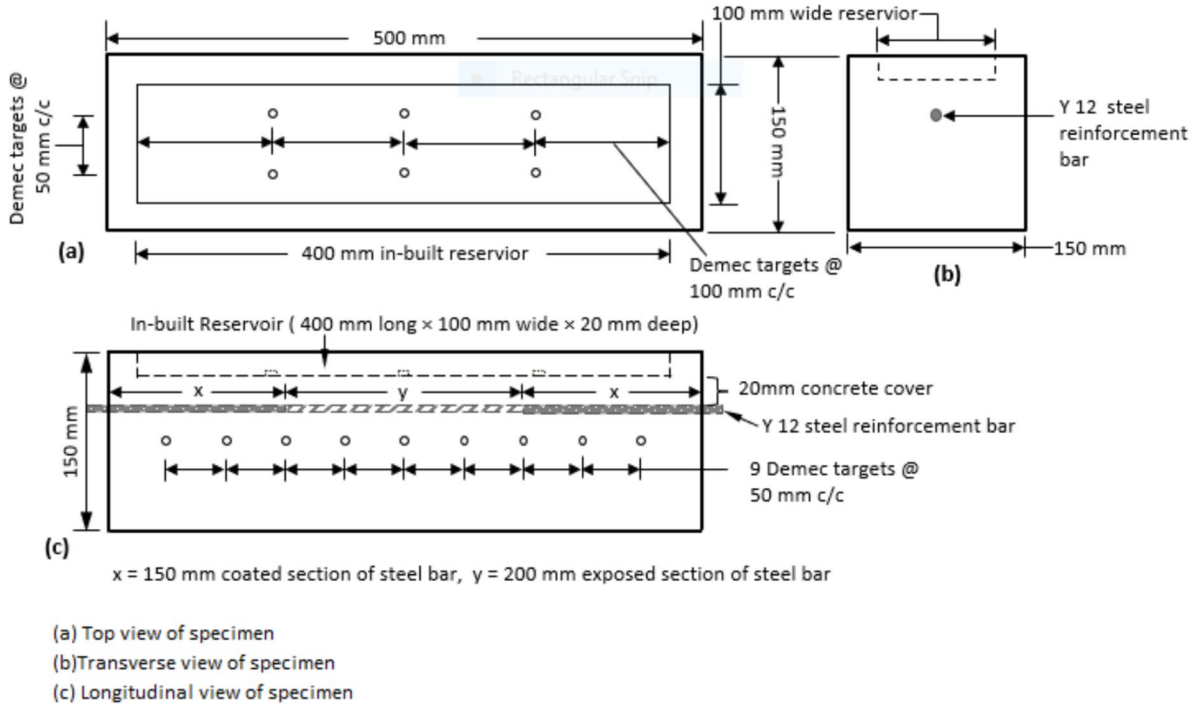

Fig. 2 **a–c** Beam specimen with embedded steel reinforcement

specimens did not have contact with the water in the storing container. After this exposure condition, the beams were exposed to cyclic 1-week wetting (in 5% NaCl solution). The 5% NaCl concentration used in this study is intended to accelerate the deterioration process, allowing to investigate the combined effects of alkali-silica reaction (ASR) and corrosion within a reasonable timeframe. This approach enables the study to evaluate the performance of different binder types under aggressive conditions.

Regarding real-world exposure conditions, the selected concentration is more representative of harsh marine environments. For de-icing salts, the concentration can vary widely depending on the application and location. However, the chosen concentration is within the range of reported values for certain de-icing salt exposures. Data from various studies support the representativeness of the chosen concentration. For example, research has shown that chloride concentrations in marine environments can range from 3.5% to over 6% in certain areas (Yilmaz et al., 2024; Otieno, 2013). By using a 5% NaCl concentration, the study aim to simulate the more aggressive end of this exposure spectrum.

This was done by ponding one face (the top face) on the specified cover depth with a chloride solution, typically using an in-built reservoir and 1-week air-drying (in an ambient laboratory environment). The reservoirs were created during the beams formwork by recessing the top exposed face of the beam specimens by 20 mm in depth, spanning the entire length of 400 mm and 100 mm width of the beam as shown in the beam sketches in Figs. 2a–c, 3. This design ensures a consistent and controlled area for chloride solution ponding.

The primary purpose of the reservoir is to prevent chloride solution leakage and ensure that chloride ions ingress only through the top exposed surface of the beam. By containing the solution within the recessed area, this minimizes potential variability in chloride ingress due to solution spillage or uneven distribution. The reservoir design does not introduce variability, as the chloride solution is evenly distributed across the exposed surface. Fig. 3 shows the sketch and photograph of the beam specimen. At the end of humid exposure, the specimens were monitored for expansion due to ASR. At the same time, the corrosion assessment tests (corrosion rate, concrete resistivity, and half-cell potential) were measured after each wetting cycle using the coulostatic technique. During the ASR and corrosion assessment tests, the laboratory was maintained at a relatively stable temperature and humidity level, typical of standard indoor conditions, and monitored using a temperature–humidity device (HT-305 m).The expansion and corrosion activity were measured for a total experimental duration of 52 weeks. The choice of a 1-year (52 weeks) exposure period also acknowledges the potential impact of seasonal variations on the

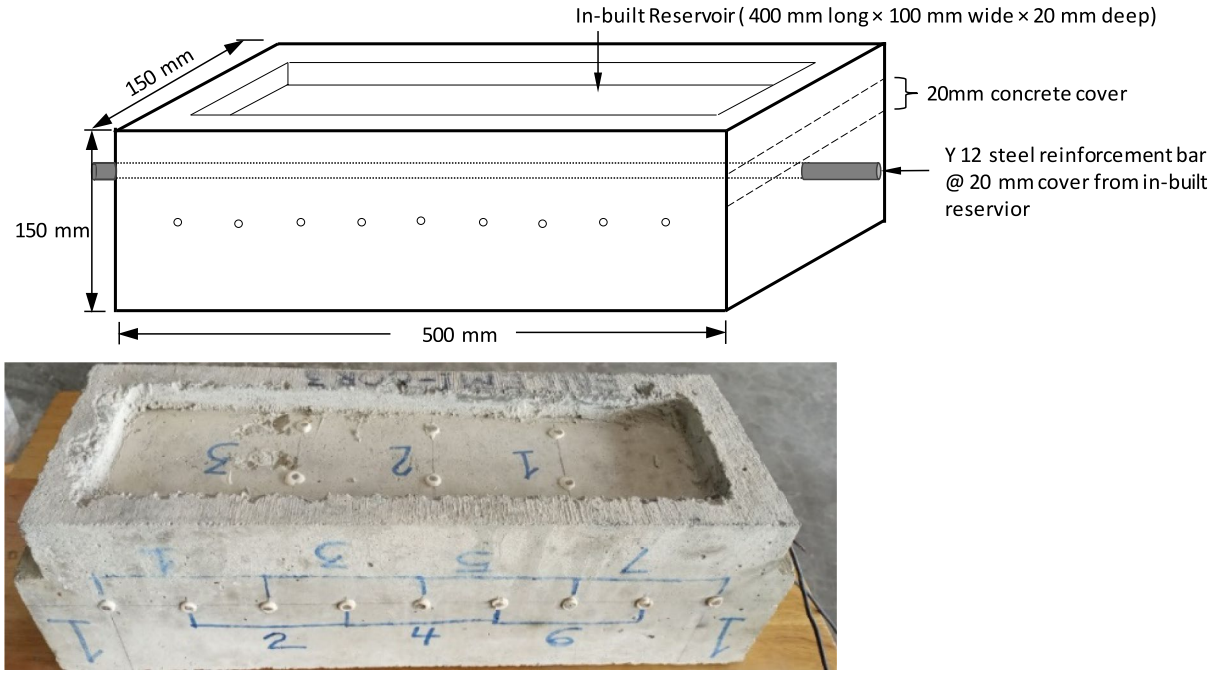

Fig. 3 Sketch and photograph of a typical 150 × 150 × 500 mm beam

durability of concrete structures, even in a laboratory setting, the prolonged duration ensures that any potential effects of minor temperature or humidity fluctuations over time are captured. This approach enables a more robust evaluation of the specimens' performance under conditions that might simulate real-world exposure scenarios. Furthermore, the 52-week duration correlates well with the progression of corrosion and expansion in the specimens. Corrosion initiation and propagation are time-dependent processes that can be influenced by various factors, including chloride ingress, moisture availability, and temperature fluctuations. By exposing the specimens to the controlled laboratory conditions for an extended period, this study was able to monitor the gradual development of corrosion and expansion, providing valuable insights into the underlying mechanisms.

2.3 Monitoring and Assessment of Corrosion and ASR-Induced Expansion

The corrosion rate was measured using a coulostatic device based on the linear polarization resistance method. This technique involves applying a known potential for a few milliseconds and monitoring the potential transient (relaxation) for approximately 50 s. The device consists of a working electrode (reinforcing steel), a reference electrode (silver–silver chloride half-cell), and a counter electrode (stainless steel).

To facilitate measurements, an electrical connection was established by attaching a wire to the steel reinforcement before casting it into the concrete. The wire was extended to the outside face of the concrete beam, allowing connection to the coulostat device.

During measurements, the concrete surface was moistened, and a damp fabric was placed over the area to ensure electrical conduction. The coulostat device was then placed over the concrete specimen, and potential measurements were taken at the end of the wetting cycle using a computer-connected setup. The corrosion rate was logged and calculated in $\mu A/cm^2$.

To quantify the expansion of concrete beam specimens due to alkali-silica reaction (ASR), DEMEC gauge studs were installed on the surface of the specimens at 50 mm intervals along the longitudinal direction and on the face of the beam specimens in the transverse direction. The DEMEC gauge was then used to measure expansion readings after exposure to humid conditions. These measurements, along with corrosion assessments, were conducted repeatedly throughout the exposure cycles to monitor the progression of ASR-induced expansion and corrosion.

3 Results and Discussion

The corrosion rate, half-cell potential, and ASR expansion data shown in this part came from beam specimens that were exposed to ASR and corrosion conditions for up to

52 weeks. Here are some examples of the notations used to show the experimental results in this paper:

- 70/30 Portland cement/fly ash contain fine reactive aggregate (PC/FA-R),
- 70/30 Portland cement/fly ash contain fine non-reactive aggregate (PC/FA-NR),
- 50/50 Portland Cement/slag contain fine reactive aggregate (PC/SL-R),
- 50/50 Portland cement/slag contain fine non-reactive aggregate (PC/SL-NR),
- 100% Portland cement contains fine reactive aggregate (PC-R), and
- 100% Portland cement contains fine non-reactive aggregate (PC-NR),

where NR represents non-reactive specimens and R represents reactive specimens.

To find out if there is a significant difference between the ASR expansion test and the corrosion assessment test, an independent two-tailed t-test with a 95% confidence range was done. A two-tailed test checks to see if the datasets being looked at are different. It is not necessary to provide a direction prior to testing. In other words, a two-tailed test looks at both the chances of a positive and a negative result.

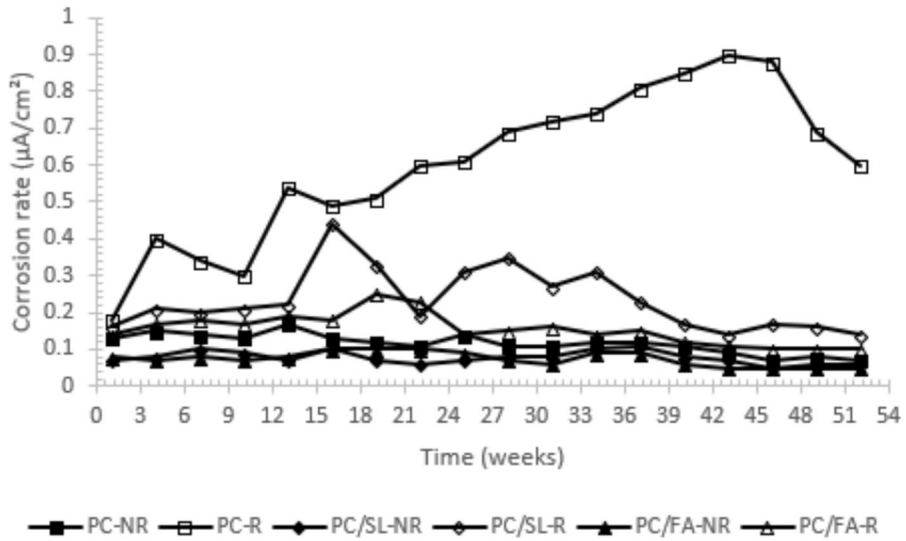

Fig. 4 Corrosion rate of all the binder types used

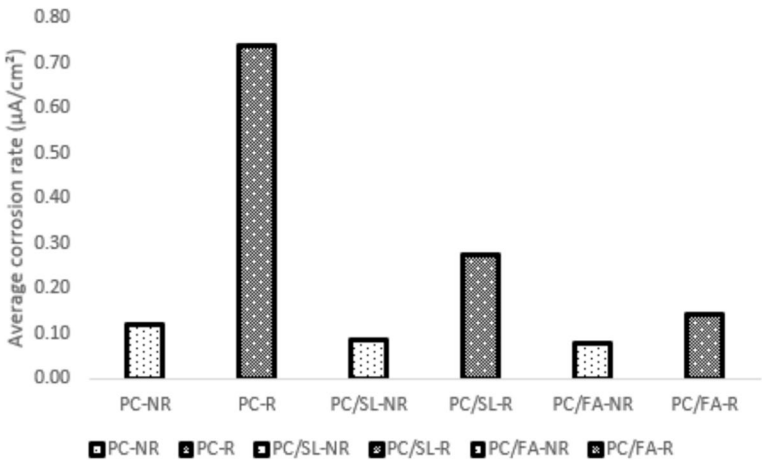

Fig. 5 Average corrosion rates for all the binder types of concrete containing reactive and non-reactive aggregate

3.1 Effect of Slag and Fly Ash on the Corrosion Rate, Corrosion Potential, and Expansion due to ASR of Concrete Made with Reactive and Non-Reactive Aggregate

3.1.1 Corrosion Rate Results

Fig. 4 shows the general trends of the corrosion rates that were measured for different binders made up of reactive and non-reactive aggregates, and Fig. 5 depicts the average corrosion rate of the different concrete specimens. The words "average corrosion rate", "average half-cell potential", and "average expansion" in this study refer to the average of the corrosion rates, expansions, and half-cell potentials that were seen between weeks 25 and 40. This time frame was chosen because the relevant parameter time–development trends, especially the corrosion rate of the concrete specimens, were in a reasonably stable phase. The selection of weeks 25–40 for calculating the average corrosion rate was based on a deliberate consideration of the corrosion process dynamics. By this period, the corrosion process had likely transitioned from the initiation stage, characterized by passive film breakdown and initial corrosion product formation, to the propagation stage, where corrosion rates tend to stabilize. By this stage, the corrosion process is likely dominated by the propagation stage, where the corrosion rate is more consistent and representative of the material's long-term behaviour. This approach is consistent with existing literature, which often focuses on steady-state corrosion rates to evaluate material performance (Zakka, 2020).

Compared to the SCMs specimens (PC/SL and PC/FA) containing fine reactive aggregate and coarse non-reactive aggregate, the control specimen (100% PC) containing fine reactive aggregate and coarse non-reactive aggregate exhibited a high corrosion rate. Even though it is anticipated that the corrosion rate for PC specimens will be higher than that of SCMs specimens, the significantly higher corrosion rate in PC specimens with reactive aggregate compared to SCMs specimens with reactive aggregate may be due to the mitigating effect of fly ash and slag on the alkali-silica reaction in the concrete. The alkali-silica reaction generates cracks and detachment at the cement paste–aggregate interface, thereby increasing the porosity of concrete (Marinoni et al., 2015). The voids and cracks formed in the concrete as a result of ASR will allow corrosive agents (Cl^-, H_2O, and O_2) to reach the surface of the steel reinforcement and maintain corrosion activity.

Even though all SCMs contain some alkali, and some may have a lot more alkali than the Portland cement they partially replace, the method by which SCMs reduce the negative effect (expansion, crack) of ASR in concrete is by reducing the alkalis that are available to the concrete pore solution. Once the alkalis in the Portland cement + SCM binding phase of concrete are "released" by hydration, they can be found in one of three ways: dissolved in the pore solution, bound by the hydration products, or mixed into alkali-silica gel. Alkalis will not be used up by ASR if there is not any reactive aggregate in the concrete (Thomas, 2011). When SCMs are used to replace Portland cement, the alkalis in the clinker are partially diluted, the rate of alkali release reduces, and the pH of the pore solution decreases. This is because $Ca(OH)_2$ has been reduced, so water cannot get into the concrete as easily, increasing the concrete's strength and making it less likely to crack (Lindgård et al., 2012). The reduced permeability will also make it harder for ions to move around, which could slow down ASR. Adding SCMs could also increase self-desiccation of the concrete, which would lead to a lower relative humidity (RH) inside the test specimens (Lindgård et al., 2012). However, monitoring the internal relative humidity of the concrete specimens was not done in this study.

The observed decline in corrosion rates across all concrete specimens as shown in Fig. 3, regardless of aggregate reactivity, can be attributed to their exposure to high humidity 94 ± 3% in a water bath. As the specimens became saturated, oxygen diffusion to the steel surface was likely hindered due to the limited solubility of oxygen in water. Although moisture content of the concrete specimens was not directly measured, the decrease in corrosion rates over time suggests that saturation occurred, potentially limiting oxygen availability and contributing to the reduced corrosion rates.

T-test analyses on the corrosion test indicate the difference in the corrosion rate of the PC concrete containing reactive aggregate to SCMs concrete containing reactive is significant—PC concrete made with reactive aggregate has a higher corrosion rate than that of the SCMs concrete containing reactive aggregate.

There was a significant difference in the corrosion rates of PC specimens compared to blended concrete (PC/SL and PC/FA) containing reactive ($p = 2.8 \times 10^{-6}$ and 2.11×10^{-7}) and non-reactive aggregate ($p = 2.67 \times 10^{-6}$ and 1.83×10^{-7}) < 0.05, respectively. This indicated that incorporating SCMs in concrete reduces the damage caused by chloride-induced steel corrosion in RC structures exhibiting an alkali-silica reaction. The higher corrosion rate in the PC-R specimen compared to the blended concretes (PC/SL-R and PC/FA-R) can be attributed to the beneficial effects of supplementary cementitious materials (SCMs) such as slag (SL) and fly ash (FA). These SCMs enhance concrete durability by creating a denser and less permeable matrix, thereby extending the service life of reinforced concrete (RC) structures. The improved microstructure of SCM-blended concrete is characterized by: (i) Denser matrix: The formation of low-density

C-S–H gel fills capillary pores, reducing porosity and increasing density (Arya & Xu, 1995; Song & Saraswathy, 2006). (ii) Reduced permeability: The refined pore structure and decreased porosity limit the ingress of corrosive agents, contributing to improved durability.

When the SCMs used in the concrete were taken into account, the PC/FA specimens had the lowest corrosion rates. Fig. 4 shows the order of the average corrosion rates of the concrete samples from week 25 to week 40: PC/FA-NR < PC/SL-NR < PC-NR < PC/FA-R < PC/SL-R < PC-R. Among the supplementary cementitious materials (SCMs) used, fly ash (FA) outperformed ground granulated blast furnace slag (SL) in reducing corrosion rates, with PC/FA specimens exhibiting the lowest rates. The presence of sulphide (3.39%, Table 2) in SL, which has oxygen-reducing properties, may have contributed to the higher corrosion rates in PC/SL specimens. The superior performance of FA concrete can also be attributed to its ability to bind chlorides, thereby reducing chloride-induced corrosion. This enhanced chloride binding capacity is likely due to the following: (i) High alumina content: Fly ash's high Al_2O_3 content (Table 2) promotes Friedel salt formation, increasing chloride binding (Arya et al., 1990). (ii) Increased gel production: Hydration-induced gel production in FA concrete enhances physical adsorption of chlorides, further improving chloride binding capacity (Rajkumar, 2014).

3.2 Corrosion Potential Results

Fig. 6 shows how the recorded corrosion potentials of different binders with reactive and non-reactive aggregate change over time, while Fig. 7 shows the average corrosion potential of the different concrete samples. According to (ASTM C876-09, 1999) guidelines and some studies (Alonso et al., 2002; Buchanan & Stansbury, 2000), values equal to or more negative than − 256 mV (Ag/AgCl) are interpreted to mean a high (˃ 90%) probability of active corrosion, which is conventionally depicted by $i_{corr} \geq 0.1$ µA/cm^2, while those less negative than − 256 mV (Ag/AgCl) are generally interpreted as intermediate corrosion risk.

Half-cell potential as a function of time over the whole testing period shows that the HCP values for reactive specimens got more negative than those for non-reactive specimens, which was expected. Notably, the corrosion rate trends for reactive specimens had a higher (more negative) HCP over time than those for non-reactive specimens. This finding matched the results of a study (Attar et al., 2020) on the properties of concrete exposed to corrosive conditions (chloride-induced steel corrosion) and showing an alkali-silica reaction. The higher (more negative) HCP found in the concrete samples with reactive aggregate may be due to how easy it was for corrosion agents to get to the reinforcing steel through the microcracks that formed when alkali and silica reacted. The chloride conductivity index (CCI) used in this study shows that concrete with reactive aggregate has higher CCI values than concrete without reactive aggregate. This means that the concrete with reactive aggregate is more porous. The findings of the CCI are shown in Table 3. This study utilized non-reactive andesite aggregate (specific gravity: 2.90) and reactive Sub-Nigel aggregate (specific gravity: 2.72). The lower specific gravity of the reactive aggregate suggests higher porosity, potentially compromising durability (Martínez-García et al., 2022). Consequently, concrete containing reactive aggregate was expected to exhibit lower resistance to chloride conductivity index (CCI).

The reactive aggregate, composed of quartz, is prone to alkali-silica reaction (ASR), which can lead

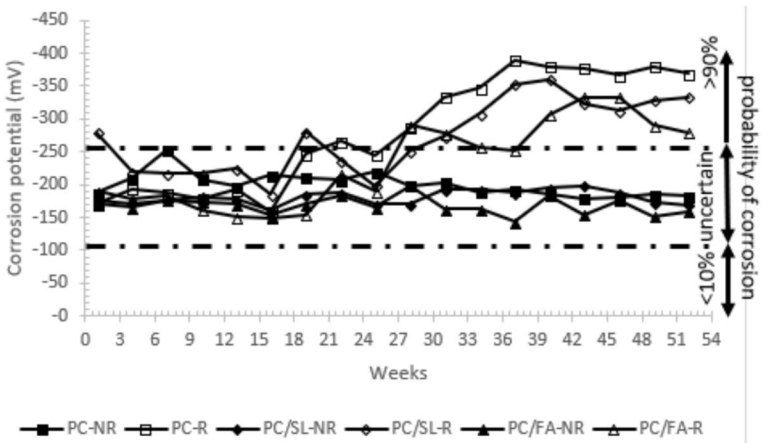

Fig. 6 Corrosion potential of all the binder types

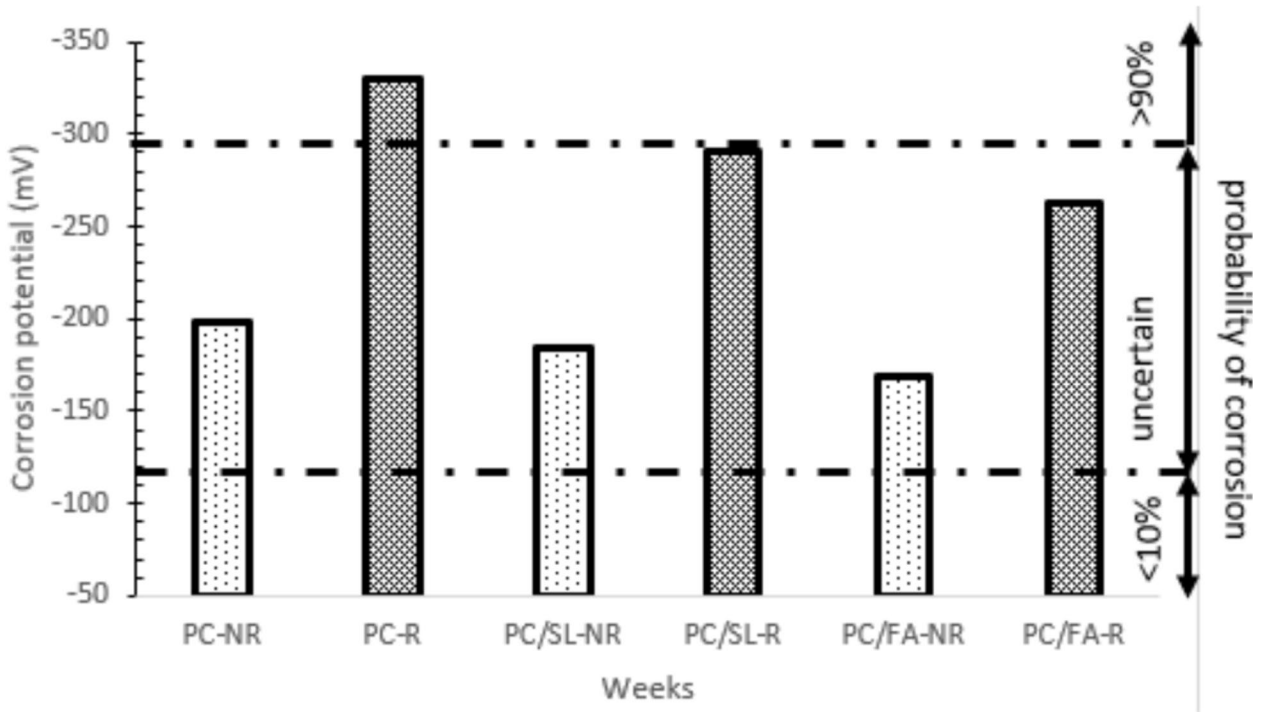

Fig. 7 Average corrosion potentials for all the binder types of concrete containing reactive and non-reactive aggregate

Table 3 CCI test results for all specimen types

Test	PC-NR	PC-R	PC/SL-NR	PC/SL-R	PC/FA-NR	PC/FA-R
CCI (mS/cm)	1.91	2.28	0.50	0.77	1.40	2.03
Porosity (%)	6.12	7.85	4.90	4.97	5.02	6.09

to void formation and increased porosity (Cruz Carlos et al.,2004; Marinoni et al., 2015). Notably, specimens with supplementary cementitious materials (SCMs) like fly ash and slag demonstrated higher resistance to chloride penetration compared to the 100% PC specimen. This suggests that the SCMs mitigated ASR's adverse effects, reducing void formation and enhancing durability.

The findings imply that the SCMs' mitigating effect on ASR-induced void formation contributed to the improved durability of concrete containing reactive aggregate. By reducing porosity, SCMs limited the ingress of corrosive agents, thereby enhancing the concrete's resistance to chloride penetration.

Compared to the PC/FA specimens, the corrosion potential of the PC/SL specimens are more negative. The reason for this trend in this study may be that concretes made with different supplementary cementitious materials (like FA and GGBS) have different effects on the corrosion activity of steel embedded in concrete because of how well they bind chlorides (Arya et al., 1990; Mackechnie, 1995). For both the reactive and non-reactive specimens, the average HCP became more negative in the following order: PC/FA-NR > PC/SL-NR > PC-NR > PC/FA-R > PC/SL-R > PC-R. This trend is similar to the average corrosion rate discussed previously.

A comparison of the average porosity values between non-reactive (NR) and reactive (R) concrete specimens reveals that the R specimens have a higher average porosity (6.30%) than the NR specimens (5.35%), with a percentage difference of 17.76%. Consistently, across all three binder types, the NR aggregate concretes exhibited lower chloride conductivity index (CCI) values than their R aggregate counterparts. This can be attributed to the reduced capillary porosity in the NR concretes, which limits ion diffusion (Sutter et al., 2008). The incorporation of supplementary binders,

such as fly ash (FA) and slag (SL), significantly reduced CCI values compared to plain Portland cement (PC) concretes. The refined pore structure and low electrical conductivity of SL concretes likely contributed to the observed trend of lower CCI values. These findings align with existing literature, which suggests that supplementary binders decrease CCI values (Mackechnie, 1995). Furthermore, FA concretes showed improved CCI values over PC concretes, likely due to pore refinement in the paste, which reduces the diffusion rate of species into the concrete (Nikam & Tambvekar, 2003).

3.3 Expansion of the Concrete Specimen due to Alkali-Silica Reaction

Figs. 8 and 9 depict the longitudinal and transverse expansion of all utilized binder varieties. All results for longitudinal and transverse expansion were presented in microstrain.

In longitudinal and transverse expansion measurements, the results showed that specimens including reactive aggregate (combined scenario) expanded significantly more than specimens containing non-reactive aggregate. This is because the reaction product (ASR gel) swells due to its attraction to absorb moisture within the concrete, resulting in concrete expansion and structural damage. There was no

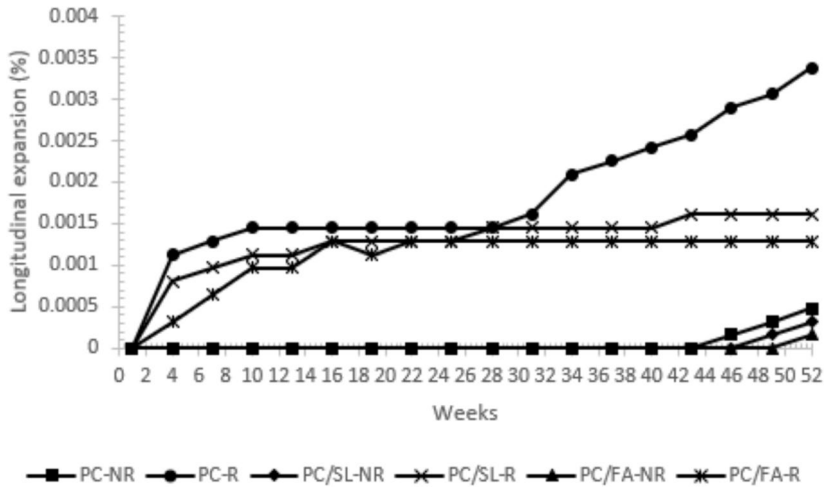

Fig. 8 Longitudinal expansion of all binder types

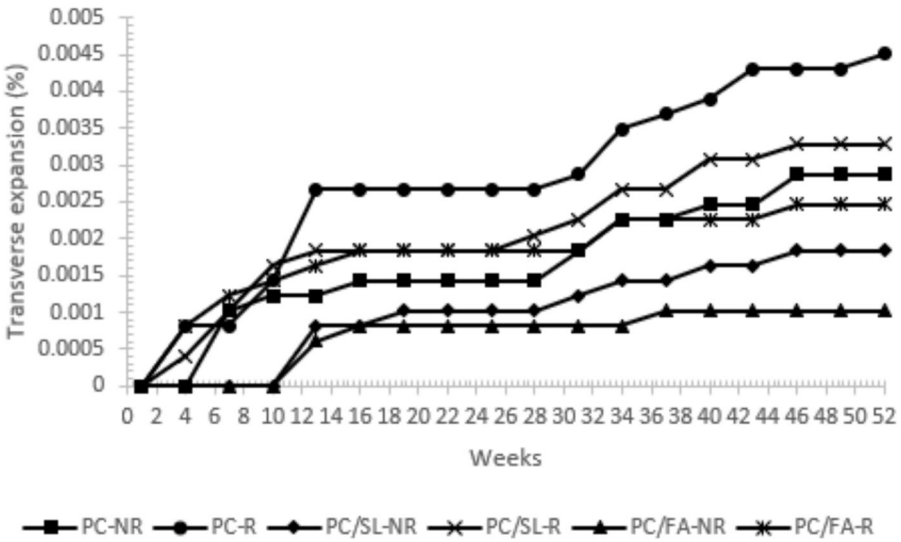

Fig. 9 Transverse expansion of all binder types

longitudinal expansion in the concrete sample that did not contain reactive aggregate. However, expansion was observed near the end of the experiment (week 46), exhibiting an unexplainable trend; the specimen exhibits the lowest (least) expansion when compared to other specimens prone to ASR in the same direction. This is due to the material hygroexpansion phenomena; moisture absorption causes a rise in the moisture content of the material as well as dimensional changes (swelling), which are thought to be proportionate to the change in moisture content. The moisture content of the specimens was not examined in this study, although it was assumed that exposure to highly humid (93.3%) conditions (storage tank) would increase the moisture content.

T-test analysis shows a significant expansion in the PC specimens containing reactive aggregate compared to the SCMs (PC/SL and PC/FA) specimens made with reactive aggregate. The results of PC-R vs SL-R and PC-R vs FA-R are ($p = 2.79 \times 10^{-4}$ and $p = 1.198 \times 10^{-4}$) < 0.05, respectively. This result indicates that including SCMs (slag and fly ash) in concrete can effectively mitigate the expansion from ASR in specimens containing fine reactive aggregate exposed to corrosive conditions. The longitudinal and transverse expansion measurements in the concrete specimen, including reactive aggregate, were not identical for the blended concretes utilized in this investigation (PC/SL and PC/FA). The PC/FA specimens expand less than the PC/SL specimens, suggesting that the FA is more effective than the GGBS in reducing the detrimental effect of the alkali-silica reaction in concrete structures. This tendency was consistent with (Parmar et al., 2019; Shi et al., 2018), and earlier research linked it to the optimal amount of fly ash required as SCM to decrease alkali-silica reaction (ASR). In comparison to other SCMs, the optimal amount of fly ash was determined to be 30%.

These results (Figs. 7 and 8) clearly demonstrate that transverse expansion increased more than longitudinal expansion. Using this analogy, we can explain why a smaller cross-sectional area is subjected to greater stress for the same force as a larger one. As an illustration, axial stress appears as follows: If there are two areas, A1 and A2, and if A1 is transverse (small) and A2 is longitudinal (large), then A1 is smaller than A2 and the force (F) is the same for both areas. This formula computes the total axial stress (S) (see Eq. 1) acting on the following regions:

$$S = \frac{F}{A}. \tag{1}$$

Due to the fact that A2 is greater than A1, the larger (longitudinal) area experiences less tension and less expansion than the smaller (transverse) area, which experiences greater expansion.

The results reveal a notable difference in expansion between plain cement (PC) specimens and those incorporating supplementary cementitious materials (SCMs), specifically PC/SL and PC/FA, when reactive aggregate is used (Figs. 7 and 8). The SCMs effectively suppress alkali-silica reaction (ASR) expansion by reducing the pore solution's alkalinity through alkali binding in hydration products (Çak, 2011; Lindgård et al., 2012).

However, exposure to NaCl solution leads to a decline in ASR-induced expansion, a trend observed around the 16th week of the experiment. This reduction is attributed to a decrease in hydroxyl ion (OH^-) concentration in the pore solution. Similar findings have been reported in previous studies (Bérubé et al., 2003; Desai, 2010; Kawamura & Ichise, 1990; Mitsunori et al., 1989), where the decrease in expansion was linked to the reduction of OH^- ions due to alkali consumption during ASR and alkali leaching from the concrete, accompanied by an increase in Cl^- ion concentration in the pore solution relative to the alkali cations.

The analysis of water samples from the specimen's storage tank, taken before the beginning of the experiment and another sample after the conclusion of the experiment, confirms alkali leaching. The hydroxyl concentration, measured using the spectrophotometer method, increased from 0.40 mmol/l to 10.2 mmol/l, indicating significant alkali leaching from the concrete specimens. This leaching reduces the hydroxyl ion concentration in the pore solution, contributing to the decreased ASR expansion.

4 Summary and Conclusion

This study examined the impact of fly ash and slag on the combined effects of alkali-silica reaction and steel corrosion in reinforced concrete structures. Cast and evaluated were eighteen (18) concrete beam specimens containing reactive and non-reactive aggregates of various binder types (100% PC, 50/50 PC/SL, and 70/30 PC/FA). This 52-week study measured corrosion assessment tests (corrosion rate and corrosion potential) and expansion at the conclusion of the wetting period and under humid conditions.

The results indicate that adding 50% and 30% SCMs (slag and fly ash) to PC in specimens with non-reactive and reactive aggregates reduces corrosion risk compared to PC specimens. In this study, Portland cement (PC) was blended with either fly ash (FA) or slag (SL) at replacement ratios commonly used in South Africa's marine concrete construction. The specific binder blends used, namely, 70/30 PC/FA and 50/50 PC/SL, have been shown in previous research to enhance protection against alkali-silica reaction (ASR) and steel corrosion

in concrete structures (Al-Saadoun et al., 1993; Otieno, 2013; Mazarei et al., 2017). To extend the service life of RC structures containing reactive aggregate in marine environments, a lower corrosion rate is advantageous. The effect of the SCMs was evident in the corrosion potential measurement, where the corrosion potential recorded for PC specimens was higher (more negative) than for SCMs specimens made with reactive and non-reactive aggregate.

The expansion measurements indicate that the addition of SCMs to the concrete mitigates the expansion caused by ASR in comparison to the specimens made with PC alone. Both specimens with reactive and non-reactive aggregate exhibited a similar pattern of outcomes. This research indicates that the percentage of PC replacement with SCMs may be optimal for slag and fly ash replacement levels to minimize corrosion rate and concrete expansion when exposed to corrosive conditions and containing reactive aggregate. Reinforced concrete (RC) structures exposed to the synergistic effects of alkali-silica reaction (ASR) and corrosion, particularly in marine environments, exhibit accelerated degradation and reduced service life compared to those subjected to either mechanism in isolation. This study investigates the coupled deterioration processes and demonstrates that strategic replacement of Portland cement (PC) with supplementary cementitious materials (SCMs) such as slag (SL) and fly ash (FA) can effectively mitigate the detrimental effects of both ASR and corrosion. The judicious selection of binder types is thus paramount in enhancing the durability of RC structures exposed to corrosive environments and susceptible to ASR-induced degradation.

Acknowledgements
The authors would like to acknowledge the assistance of the University of the Witwatersrand in providing the laboratory facilities and the support of the Concrete Material Research Unit, Department of Civil Engineering, University of the Witwatersrand. The corresponding author also extends special thanks to the Tertiary Education Trust Fund (TET Fund), Nigeria, for their support.

Author contributions
Dr. Williams Dunu was involved in conceptualization, methodology, writing—original draft, investigation, data analysis, and writing—review and editing. Prof. Mike Otieno performed supervision.

Funding
This research did not receive any specific grant from funding agencies in the public, commercial, or not-for-profit sectors.

Availability of data and materials
The data used for this study are available upon request from the corresponding author. However, the material specimens used in the experimental investigation were destroyed at the end of the experiment. This was necessary to remove the embedded steel from the concrete beam specimens, which involved breaking the beams to record the corroded steel mass loss. The results of this investigation will be utilized in a future publication.

Declarations

Ethics approval and consent to participate
Not applicable, as this study does not involve human subjects.

Consent for publication
The authors consent to the publication of this manuscript.

Competing interests
The authors declare that they have no competing interests.

Received: 6 March 2025 Accepted: 1 June 2025
Published online: 10 November 2025

References

Afrisam South Africa Pty (Ltd). (2017). *AfriSam technical reference guide*. (8th Edition). Promise.

Alonso, C., Castellote, M., & Andrade, C. (2002). Chloride threshold dependence of pitting potential of reinforcements. *Electrochimica Acta, 47*(21), 3469–3481. https://doi.org/10.1016/S0013-4686(02)00283-9

Al-Saadoun, S. S., Rasheeduzzafar, X., & Al-Gahtani, A. S. (1993). Corrosion of reinforcing steel in fly ash blended cement concrete. *Journal of Materials in Civil Engineering, 5*(3), 356–371. https://doi.org/10.1002/9780470114735.hawley07452

Angulo-Ramírez, D. E., Mejía de Gutiérrez, R., & Medeiros, M. (2018). Alkali-activated Portland blast furnace slag cement mortars: Performance to alkali-aggregate reaction. *Construction and Building Materials, 179*, 49–56. https://doi.org/10.1016/j.conbuildmat.2018.05.183

Arya, C., Buenfeld, N. R., & Newman, J. B. (1990). Factors influencing chloride-binding in concrete. *Cement and Concrete Research, 20*(2), 291–300. https://doi.org/10.1016/0008-8846(90)90083-A

Arya, C., & Xu, Y. (1995). Effect of cement type on chloride binding and corrosion of steel in concrete. *Cement and Concrete Research, 25*(4), 893–902. https://doi.org/10.1016/0008-8846(95)00080-V

ASTM C227-03. (1994). Standard Test Method for Potential Alkali Reactivity of Aggregates (Mortar-Bar. *Test*, 04, pp. 4–7. Available at: https://doi.org/10.1520/C1260-07.2

ASTM C876-09. (1999). Standard Test Method for Half-Cell Potentials of Uncoated Reinforcing. 03(Reapproved), pp. 1–6.

ASTM Standard C1293. (2008). Standard Test Method for Determination of Length Change of Concrete Due to Alkali- Silica Reaction. *ASTM International*, pp. 1–6. Available at: https://doi.org/10.1520/C1293-18.2

Attar, A., Gencturk, B., Aryan, H., & Wei, J. (2020). Impact of laboratory-accelerated aging methods to study alkali-silica reaction and reinforcement corrosion on the properties of concrete. *Materials, 13*(15), 1–27. https://doi.org/10.3390/MA13153273

Bérubé, M. A., Dorion, J. F., Duchesne, J., Fournier, B., & Vezina, D. (2003). Laboratory and field investigations of the influence of sodium chloride on alkali-silica reactivity. *Cement and Concrete Research, 33*(1), 77–84. https://doi.org/10.1016/S0008-8846(02)00926-2

Buchanan, R.A. and Stansbury, E.E. (2000). Fundamentals of electrochemical corrosion. ASM International. Available at: https://www2.arnes.si/~bzajec/kor_knj/Fundamentals%20of%20Electrochemical%20Corrosion_Stansbury,%20Buchanan_2000.pdf

Çak, A. (2011). Alkali-silica reactions (ASR): Literature review on parameters influencing laboratory performance testing. *Cement and Concrete Research, 42*(2), 44.

Cho, M.-S., & Noh, J.-M. (2012). Assessment of properties and durability of fly ash concrete used in korean nuclear power plants. *Nuclear Engineering and Technology, 44*(3), 331–342. https://doi.org/10.5516/NET.09.2010.031

Cruz, C. Mauricio Mancio, K.S. (2004). *Accelerated Laboratory Testing for Alkali-Silica Reaction Using ASTM 1293 and Comparison with ASTM 1260, UC Pavement Research Center*. Available at: http://www.ucprc.ucdavis.edu/PublicationsPage.aspx

Desai, P. (2010). *Alkali silica reaction under the influence of chloride based deicers*. Clemson University.

Fang, C., Gylltoft, K., & Karin Lundgren, M. P. (2006). Effect of corrosion on bond in reinforced concrete under cyclic loading. *Cement and Concrete Research, 36*(3), 548–555. https://doi.org/10.1016/j.cemconres.2005.11.019

Heisig, A., Urbonas, L., Beddoe, R. E., & Heinz, D. (2016). Ingress of NaCl in concrete with alkali reactive aggregate: Effect on silicon solubility. *Materials and Structures/materiaux Et Constructions, 49*(10), 4291–4303. https://doi.org/10.1617/s11527-015-0788-y

Kawamura, M., & Ichise, M. (1990). Characteristics of alkali-silica reaction in the presence of sodium and calcium chloride. *Cement and Concrete Research, 20*(5), 757–766. https://doi.org/10.1016/0008-8846(90)90009-M

Khanzadeh-Moradllo, M., Meshkini, M. H., Eslamdoost, E., Sadati, S., & Shekarchi, M. (2015). Effect of wet curing duration on long-term performance of concrete in tidal zone of marine environment. *International Journal of Concrete Structures and Materials, 9*(4), 487–498. https://doi.org/10.1007/s40069-015-0118-3

Kim, T., & Olek, J. (2016). The effects of lithium ions on chemical sequence of alkali-silica reaction. *Cement and Concrete Research, 79*, 159–168. https://doi.org/10.1016/j.cemconres.2015.09.013

Leemann, A., et al. (2014). Mitigation of ASR by the use of LiNO3—Characterization of the reaction products. *Cement and Concrete Research, 59*, 73–86. https://doi.org/10.1016/j.cemconres.2014.02.003

Liaudat, J., et al. (2018). ASR expansions in concrete under triaxial confinement. *Cement and Concrete Composites, 86*, 160–170. https://doi.org/10.1016/j.cemconcomp.2017.10.010

Lindgård, J., et al. (2012). Alkali-silica reactions (ASR): Literature review on parameters influencing laboratory performance testing. *Cement and Concrete Research, 42*(2), 223–243. https://doi.org/10.1016/j.cemconres.2011.10.004

Liu, K.-W., et al. (2018). Chemical approaches to prevent alkali-silica reaction in concrete—A review. *Engineering Solid Mechanics, 6*, 201–208. https://doi.org/10.5267/j.esm.2018.6.003

Mackechnie, J.R. (1995). Predictions of reinforced concrete durability in the marine environment, Department of civil engineering, University of Cape Town. Cape Town.

Marinoni, N., et al. (2015). A combined synchrotron radiation micro computed tomography and micro X-ray diffraction study on deleterious alkali-silica reaction. *Journal of Materials Science, 50*(24), 7985–7997. https://doi.org/10.1007/s10853-015-9364-7

Martínez-García, R., Sanchez de Rojas, M. I., Jagadesh, P., Lopez-Gayarre, F., Moran-del-Pozo, J. M., & Juan-Valdes, A. (2022). Effect of pores on the mechanical and durability properties on high strength recycled fine aggregate mortar. *Case Studies in Construction Materials, 16*, 1–23. https://doi.org/10.1016/j.cscm.2022.e01050

Mazarei, V., Trejo, D., Ideker, J. H., & Isgor, O. B. (2017). Synergistic effects of ASR and fly ash on the corrosion characteristics of RC systems. *Construction and Building Materials, 153*, 647–655. https://doi.org/10.1016/j.conbuildmat.2017.07.097

Mitsunori, K., Kunio, T., Makoto, I. (1989). Influence of the alkali-silica reaction on the corrosion of steel reinforcement in concrete. in and M.K. K. Okada, S. Nishibayashi (ed.) *8th International Conference on Alkali-Aggregate Reaction*. Japan: 8th ICAAR Local Organizing Committee. The Society of Materials Science, pp. 881–885.

Nikam, V.S. and Tambvekar, V.Y. (2003). Effect of Different Supplementary Cementitious Material on the Microstructure and its Resistance Against Chloride Penetration of Concrete Effect of Different Supplementary Cementitious Material on the Microstructure and its Resistance Against Chloride Pen. *Advanced Materials for Construction of Bridges, Buildings, and Other Structures III*, pp. 1–10.

Otieno, M.B. (2013). *The Development of Empirical Chloride-induced corrosion Rate Prediction Models for Cracked and Uncracked Steel Reinforced Concrete Structures in the Marine Tidal Zone*. University of Cape Town. Available at: https://open.uct.ac.za/handle/1142/9520.

Otieno, M. B., Alexander, M. G., & Beushausen, H.-D. (2010). Corrosion in cracked and uncracked concrete—Influence of crack width, concrete quality and crack reopening. *Magazine of Concrete Research*. https://doi.org/10.1680/macr.2010.62.6.393

Parmar, H. S., Gupta, T., & Sharma, R. K. (2019). A critical review on mitigation of alkali-silica reaction in concrete. *International Journal of Engineering Science Invention, 8*, 34–40.

Rajkumar, V. (2014). Corrosion resistance performance of ethylamines in fly ash blended cement concrete. *Applied Mechanics and Materials, 507*, 286–290. https://doi.org/10.4028/www.scientific.net/AMM.507.286

Rutkauskas, A., Nagrockiene, D., & Skripkiunas, G. (2017). Cement type influence on alkali-silica reaction in concrete with crushed gravel aggregate. *IOP Conference Series: Materials Science and Engineering, 251*(1), 8–16. https://doi.org/10.1088/1757-899X/251/1/012032

Saha, A. K., et al. (2018). The ASR mechanism of reactive aggregates in concrete and its mitigation by fly ash: A critical review. *Construction and Building Materials, 171*, 743–758. https://doi.org/10.1016/j.conbuildmat.2018.03.183

SANS 920: 2011. (2011). South African National Standard: Steel bars for concrete reinforcement.

Shi, Z., et al. (2018). Alkali-silica reaction in waterglass-activated slag mortars incorporating fly ash and metakaolin. *Cement and Concrete Research, 108*(2017), 10–19. https://doi.org/10.1016/j.cemconres.2018.03.002

Song, H. W., & Saraswathy, V. (2006). Studies on the corrosion resistance of reinforced steel in concrete with ground granulated blast-furnace slag—An overview. *Journal of Hazardous Materials, 138*(2), 226–233. https://doi.org/10.1016/j.jhazmat.2006.07.022

Sutter, L. et al. (2008). The deleterious chemical effects of concentrated deicing solutions on Portland cement concrete. *South Dakota Department of Transportation Office of Research*, 5(April), p. 216. Available at: http://www.michiganltap.org/sites/ltap/files/workshops/materials/a_darker_side_of_anti_icing_chemicals.pdf

Thomas, M. (2011). The effect of supplementary cementing materials on alkali-silica reaction: A review. *Cement and Concrete Research, 41*(12), 1224–1231. https://doi.org/10.1016/j.cemconres.2010.11.003

Torres-Luque, M., et al. (2014). Non-destructive methods for measuring chloride ingress into concrete: State-of-the-art and future challenges. *Construction and Building Materials, 68*, 68–81. https://doi.org/10.1016/j.conbuildmat.2014.06.009

Trejo, D., Mazarei, V., Ideker, J. H., & Isgor, O. B. (2017). Influence of alkali-silica reaction reactivity on corrosion in reinforced concrete. *ACI Materials Journal, 114*(5), 723–731. https://doi.org/10.14359/51689895

Williamson, T., & Juenger, M. C. G. (2016). The role of activating solution concentration on alkali-silica reaction in alkali-activated fly ash concrete. *Cement and Concrete Research, 83*, 124–130. https://doi.org/10.1016/j.cemconres.2016.02.008

Yilmaz, D., Rossi, E., & Angst, U. (2024). Assessment of corrosion attack morphology on reinforced concrete structures exposed to chlorides. *Structural Concrete*. https://doi.org/10.1002/suco.202401161

Zakka, Z.G. (2020) *Influence of two-directional ingress of corrosion agents on the initiation and propagation of steel corrosion in concrete*. University of the Witwatersrand.

Publisher's Note

Dr. Williams Dunu is an Assistant Professor in the Department of Civil Engineering at Nusa Putra University, Indonesia. He holds a Bachelor's and Master's degrees from Ahmadu Bello University, Zaria, Nigeria, and a PhD in Civil Engineering from the University of the Witwatersrand (WITS), Johannesburg, South Africa. He is a Senior Member of the International Union of Laboratories and Experts in Construction Materials, Systems, and Structures (RILEM). He received the Award of Excellence and Innovation in Research in the School of Civil and Environmental Engineering at WITS University in 2023. His research interests focus on the durability and longevity of reinforced concrete structures, as well as the assessment, repair, and maintenance of deteriorating concrete structures affected by steel corrosion and alkali-silica reaction.

Mike Otieno is a Chartered Engineer (UK), a Senior Fellow of the Higher Education Academy, and Senior Lecturer in Reinforced Concrete Structures in the School of Physics, Engineering and Computer

Science at the University of Hertfordshire, UK. He received his PhD and MSc (Eng) degrees from the University of Cape Town, South Africa, and a First Class Honours BSc (Civil Eng.) degree from the University of Nairobi, Kenya. He also holds a Postgraduate Diploma in Education (in Higher Education, with Distinction) from the University of the Witwatersrand, Johannesburg. His teaching covers both undergraduate and postgraduate courses in Construction Materials, including Strength/Mechanics of Materials. His research interests include concrete durability, service life prediction, steel corrosion in reinforced concrete structures and repair and rehabilitation of concrete structures.